Journal of Physics: Conference Series

PAPER • OPEN ACCESS

Calculation and Experimental Study on a Rotary Percussion Positive Displacement Motor

To cite this article: Haiping Zhang *et al* 2020 *J. Phys.: Conf. Ser.* **1626** 012100

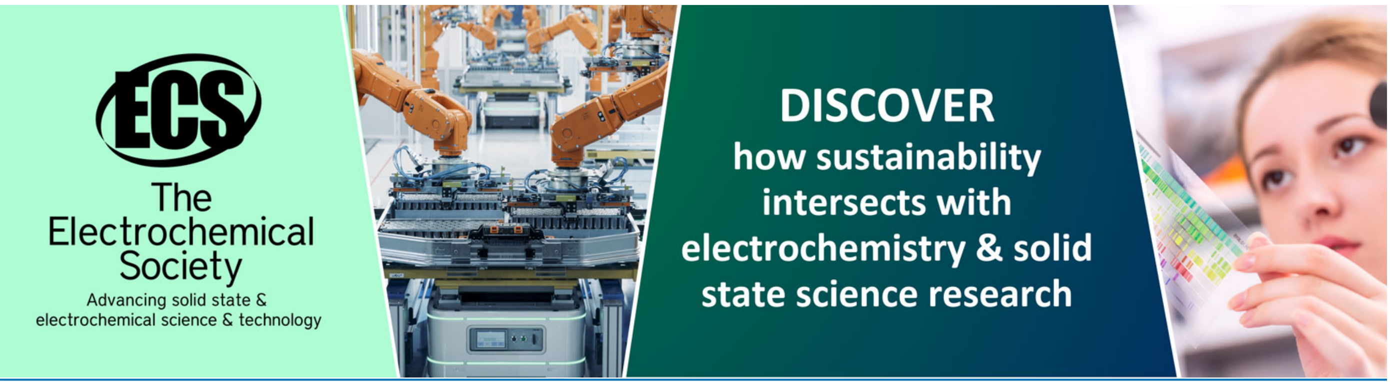

Calculation and Experimental Study on a Rotary Percussion Positive Displacement Motor

Haiping Zhang*, Yanbin Zang and Jiachang Wang

Sinopec Research Institute of Petroleum Engineering, Beijing, 100101, China

*Corresponding author email: zhangypsripe@sinopec.com

Abstract. A positive displacement motor (PDM) driven rotary percussion drilling tool, named rotary percussion PDM (RP PDM), is developed. Using conventional PDM as rotating power source, high-frequency axial impact and vibration or impact is generated to raise rate of penetration (ROP) through an impact mechanism consisting of a couple of mating cams. Strength is calculated and checked for dangerous cross-sections, and all of them meet the strength requirements. Stress distribution under different loads is analysed for the mating cam mechanism. Safety coefficients of upper and lower cams under maximum load are 3.69 and 2.36 respectively. Both are greater than the allowable safety coefficients, which prove tool's design safety and reliability. Ground performance test shows that its overall power output parameters meet field compound drilling condition requirements. Field trials shows preferable ROP improving effect by over 30%. In Xu36A well especially, ROP is more than doubled. Therefore, the tool has positive significance to accelerate the pace of oil exploration and development and to reduce drilling costs.

Keywords: Rotary percussion PDM; Impact generating mechanism; Strength calculation; Finite element analysis; Experimental research.

1. Introduction

Over the years, researches [1,2] and experiments have proven that rotary percussion drilling technology [3] is one of the effective methods to increase drilling speed in deep and hard strata and that it has been continuously developing since its birth. After that various ROP improving tools spring up, like self-propelled swirling jet bit [4], hydraulic impact tool [5,6] and impulsive devices [7,8].

Two decades ago, Sinopec developed a kind of hydro-efflux hammer and did a lot of researches, like on rotary percussive technology [9], tool design and experiments [10-12], failure analyses [13-16] and applications [17] etc. It has gone through over 40 trials, with ROP improvement of above 30%. However, like most other rotary percussion drilling tools, many problems exist, such as short tool lifetime, immature technology etc. which is why rotary percussion drilling tools have not been industrialized.

PDM driven rotary percussion drilling tool is a new type of axial impact drilling tool coming up these years. The most representative ones are Torkbuster [18,19] from United Diamond Corporation and Fluid hammer from NOV. This kind of tools integrate functions of both positive displacement motor and impact hammer, and achieve good ROP improving effect. But currently, the technology is not mature yet and there is still a gap between downhole tools' working stability and field requirements.

Years ago, Sinopec Research Institute of Petroleum Engineering explored and developed a rotary percussion drilling tool [20-22], combining technologies of PDM compound drilling [23,24] and rotary percussion drilling [25,26]. The tool uses a positive displacement motor as the driving force to produce high-frequency axial impact through its impact mechanism, consequently, the co-effect of high speed rotation and high frequency impact is achieved. High rotating speed means high cutting speed, and high frequency impact means high rock crushing frequency. Therefore, rock breaking efficiency is increased and ROP is improved. In addition, the tool structure is simple. It doesn't contain springs, rubbers or any other vulnerable parts, and has a longer service life.

2. Structure and Working Principle of RP PDM

RP PDM includes two parts, a specially manufactured conventional PDM and an impact generator, and it combines the functions of the two parts to further increase drilling efficiency. The drilling fluid drives the PDM to rotate the drill bit. Meantime, the PDM uses part of the rotating energy to drive the cam follower to go up and down through an impact generator consisting of a mating cam. During the downward process, under the force of its own weight, the cam follower impacts the anvil block, which then transmits the impact energy to the drill bit. Reciprocating like this, the tool produces high frequency axial impact. High frequency axial impact combining high speed rotation is equivalent to high frequent rock breaking process, which as a result improves ROP greatly. The tool structure is shown in figure 1.

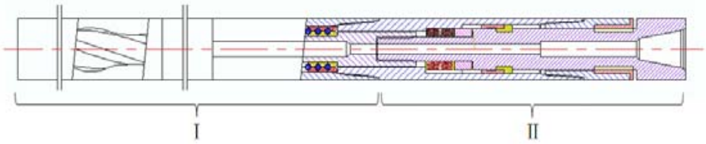

I. Specially manufactured PDM; II. Impact generator

Figure 1. Structure drawing of the RP PDM.

3. Strength Checking Calculation and Analysis of RP PDM

RP PDM's dangerous cross-sections are analysed and strength checking calculation are carried out based on the Strength check theories of *the Third Strength Theory, the Compressive Stress Condition and the Extrusion Stress Condition*, etc. If all dangerous cross-sections meet strength requirements, the tool's design parameters are feasible and its overall structure is settled accordingly.

3.1. Load Selection

According to real drilling conditions, the follow load parameters are selected. Maximum weight on bit is $\mathrm{P_{max}} = 200\ \mathrm{kN} = 20000\mathrm{kgf}$, and maximum torque is $\mathrm{M_{max}} = 20\ \mathrm{kN \cdot m} = 2000\mathrm{kgf \cdot m}$. With the loads treated as pulsating, cyclical characteristic parameter is selected as $\mathrm{r} = 0$. Then, average weight on bit is $\mathrm{P_m} = 100\ \mathrm{kN}$, and load amplitude is $\mathrm{P_a} = 100\ \mathrm{kN}$. Average torque is $\mathrm{M_m} = 10\ \mathrm{kN \cdot m}$, and torque amplitude is $\mathrm{M_a} = 10\ \mathrm{kN \cdot m}$.

3.2. Selection of Dangerous Cross-sections

Through analysis, the following are dangerous cross-sections, seen in figure 2.

Cross-section I locates at the thread root of impact generator outer shell and the motor output shaft connection, while Cross-section VI at the thread root of the impact generator outer shell and the lower joint connection. These two cross-sections are calculated according to the *Third Strength Theory*.

Cross-section II of the lower cam spline and cross section IV of the upper cam spline need to be checked for torque transmitting capacity.

The lower cam spline's smallest diameter cross-section III and the upper cam spline's smallest diameter cross section IV need to be checked for axial compression bearing capacity.

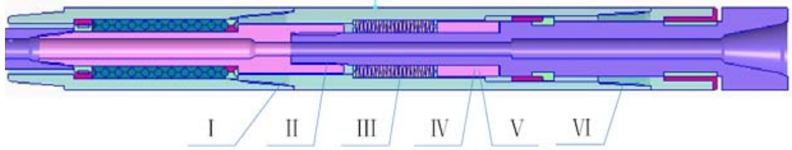

Figure 2. Distribution of dangerous section.

3.3. Strength Calculation and Analysis

(A) Strength check of cross-section I and VI

Tool diameter is $D = 178$ mm. Cross-section I locates at 1/3 distance of its thread length to the root with diameter of $d_1 = 140.7814$ mm. While cross-section VI locates at 1/3 distance of its thread length to the root with diameter of $d_6 = 147.738$ mm.
Material is 42CrMoA, thermally refined. Its allowable safety coefficient is 2.5~3, tensile strength is $\sigma_b = 110\frac{\text{kgf}}{\text{mm}^2} = 1080MPa$, and yield strength is $\sigma_s = 95\frac{\text{kgf}}{\text{mm}^2} = 930MPa$.
(1) Check according to *the Third Strength Theory*

$$\text{Area formula: } A = \pi(D^2 - \text{d}^2)/4 \tag{1}$$

$$\text{Tensile stress formula:} \sigma = P_{\max}/A \tag{2}$$

$$\text{Torsion section modulus:} W = \pi(D^4 - d^4)/(16 \times D) \tag{3}$$

$$\text{Shear stress: } \tau = M_{\max}/W \tag{4}$$

$$\text{Equivalent stress: } \sigma_{\text{xd}} = 1/2(\sigma^2 + 4\tau^2) \tag{5}$$

$$\text{Safety coefficient: } n = \sigma_s/\sigma_{\text{xd}} \tag{6}$$

By substituting the section parameters into the calculation formulas $n_1 = 15.055$, $n_6 = 12.936$, and both are greater than the allowable safety coefficient. So the two cross-sections are safe under equivalent stress.
(2) Fatigue strength check combining compression and torsion effect
With the loads treated as pulsating, cyclical characteristic parameter is $r = 0$. Stress amplitude is $\sigma = \sigma_a/2$ and $\tau_a = \tau/2$. Average stress is $\sigma_m = \sigma/2$ and $\tau_m = \tau/2$.
①Fatigue safety coefficient formula under pure compressive stress:

$$n_\sigma = \sigma_{-1}/[K_\sigma \times \sigma_a/(\varepsilon_\sigma \times \beta) + \psi_\sigma \times \sigma_m] \tag{7}$$

Referring to relative table [27] and the mechanical design manual, the following data is selected, $\sigma_{-1} = 0.23(\sigma_b + \sigma_s) = 0.23(110 + 95) = 47.15$, $K_\sigma = 2.58$, $\varepsilon_\sigma = 0.54$, $\beta = 0.85375$ and $\psi_\sigma = 0.2$. Substituting above data into formula (7), pure compressive fatigue safety coefficient of cross-section I is obtained as $n_{\sigma 1} = 7.481$, and pure compressive fatigue safety coefficient of cross-section Ⅵ is $n_{\sigma 6} = 6.227$.
② Fatigue safety coefficient formula under pure torsional stress:

$$n_\tau = \tau_{-1}/[K_\sigma \times \tau_a/(\varepsilon_\tau \times \beta) + \psi_\tau \times \sigma_m] \tag{8}$$

Referring to relative table [27], the following data is ascertained, $\tau_{-1} = 0.156(\sigma_b + \sigma_s) = 0.156(110 + 95) = 31.98$, $K_\sigma = 2.58$, $\varepsilon_\tau = 0.60$, $\beta = 0.85375$ and $\psi_\tau = 0.1$. Substituting above data into formula (8), pure torsional fatigue safety coefficient of cross-section I is obtained as $n_{\tau 1} = 4.197$, and pure torsional fatigue safety coefficient of cross-section VI is $n_{\tau 6} = 3.623$.
③ Fatigue safety coefficient combining compressive and torsional stress:

$$n_{\sigma\tau} = n_\sigma \times n_\tau/({n_\sigma}^2 + {n_\tau}^2)^{1/2} \tag{9}$$

By substituting results of formulas (7) and (8) into formula (9), the combined compressive and torsional fatigue safety coefficient of cross-section I is $n_{\sigma\tau 1} = 3.66$, and that of cross-section VI is $n_{\sigma\tau 6} = 3.13$. Both are greater than the allowable safety coefficient, therefore these two cross-sections are designed safe.
(B) Spline torque transmitting capacity check of cross-sections II and IV
The main function of the spline shaft is to offset the torque. It is assumed that the load is uniformly distributed along the spline length and that the net resultant force N of the pressure on each tooth surface acts on the average diameter of the spline shaft. Then *the Extrusion Strength Condition* is as follows,

$$\sigma_p = 2M/(\varphi zhld_m) \leq [\sigma]_p \tag{10}$$

Where, M- spline torque, kN·m; φ- The coefficient of uneven pressure distribution between the tooth surfaces in connection, usually taken φ=0.7~0.8; h- Height of tooth contact surface (working height of

tooth), m; z- Spline teeth number; l- Length of contact surface of tooth (working length of tooth), m; d_m- Average diameter of spline joint, m; $[\sigma]_p$- Allowable compressive stress on the side of the tooth (allowable specific pressure), Mpa; σ_p - Spline material allowable compression stress, Mpa.
The height and length of the spline contact surface are calculated by the following formulas:

$$h = (D - d)/2 - 2f \tag{11}$$

$$d_m = (D + d)/2 \tag{12}$$

Where, D- spline outer diameter, m; d- Spline inner diameter, m; f- Spline tooth chamfering distance, m.
Substitute the following data of cross-section II including $M = 20\ \mathrm{kN \cdot m}$, $\varphi = 0.7$, $z = 8$, $D_2 = 68\ \mathrm{mm}$, $d_2 = 62\ \mathrm{mm}$, $f_2 = 1\ \mathrm{mm}$, $l_2 = 80\ \mathrm{mm}$ into formulas(10), (11) and (12), we get $\sigma_{p2} = 1.37\ \mathrm{MPa}$.
Substitute the following data of cross-section V including $M = 20\ \mathrm{kN \cdot m}$, $\varphi = 0.7$, $z = 3$, $D_4 = 140\ \mathrm{mm}$, $d_4 = 120\ \mathrm{mm}$, $f_4 = 1\ \mathrm{mm}$, $l_4 = 120\ \mathrm{mm}$ into formulas(10), (11) and (12), we get $\sigma_{p4} = 0.15\ \mathrm{MPa}$.
The spline shaft material is 42CrMoA hardened. It can be seen that the allowable compressive stress of the two spline shafts is far smaller than the yield strength of 930 MPa. The spline shaft meets *the Extrusion Strength Condition*, so these two cross-sections are designed safe.

(C)Axial compression bearing capacity check of cross-sections III and V

In order to ensure rotary percussion safety, the tool must be strong enough. Since the upper and lower cams of the impact mechanism are the main parts to bear weight on bit, which directly acts on the upper and lower cam's axles, axial compression bearing capacity needs to be checked for the two cross-sections located here. Calculation is carried out based on the maximum downhole axial pressure 180kN. Relevant calculation formulas are as follows.
Axial stress and area are,

$$\sigma = P/S \tag{13}$$

$$S = \pi(D_0^2 - D_1^2)/4 \tag{14}$$

Where, S-area of cross-section, m; P-axial load, N; D_o- Cam axle outside diameter, m; D_1- Cam axle inner diameter, m.
Take the known parameters of the lower cam shaft like $D_{\mathrm{o}3} = 70\ \mathrm{mm}$, $D_{\mathrm{i}3} = 30\ \mathrm{mm}$, and $P_{\max} = 200\ \mathrm{kN}$ into formulas (13) and (14), the maximum tensile stress of the lower cam is obtained as $\sigma_{max3} = P_{max}/S = 63.66\mathrm{MPa}$.
Take the known parameters of the upper cam shaft like $D_{\mathrm{o}5} = 120\ \mathrm{mm}$, $D_{\mathrm{i}5} = 100\ \mathrm{mm}$, and $P_{\max} = 200\ \mathrm{kN}$ into formulas (13) and (14), maximum tensile stress of the upper cam is obtained as.$\sigma_{max5} = P_{max}/S = 57.87\mathrm{MPa}$.
The cams' material is 42CrMoA, whose yield strength is 930 MPa. Take the safety coefficient as $n = 3$. Then the allowable stress is $[\sigma] = \sigma_s/n = 310\mathrm{MPa}$. Since the maximum tensile stress σ_{max3} of the lower cam and maximum tensile stress σ_{max5} of the upper cam are both smaller than the allowable stress $[\sigma]$, the cam axles meet the Compressive Stress Condition. Therefore, these two cross-sections are designed safe, also.
Since all dangerous cross-sections meet strength requirements, the tool's structural design parameters are proved feasible.

4. Ground Performance Test

A RP PDM engineering prototype is developed. In order to open the RP PDM's operative mode, ground testing rig's circulation system is reconstructed by setting spring devices at the tool's drain back-end. After all is prepared, pump pressure, torque, and rotating speed of conventional PDM and RP PDM are tested under condition of 20 kN spring force on ground testing rig [28,29], seen in figure 3.

Figure 3. Conventional PDM and RP PDM ground testing rig.

Pump pressure, torque and rotating speed comparison for conventional PDM and RP PDM is carried out, which is shown in figure 4 and figure 5 separately. It can be seen from figure 4 that the two curves follow the same regular linear positive pattern, with fitting formulas of $y = 0.2x + 1.58$ and $y = 0.2 - 3.08$ respectively, and that pump pressure of RP PDM is 1.5MPa higher than the conventional PDM. The results certifies the following conclusion that the RP PDM's output performance parameters meet design requirements.

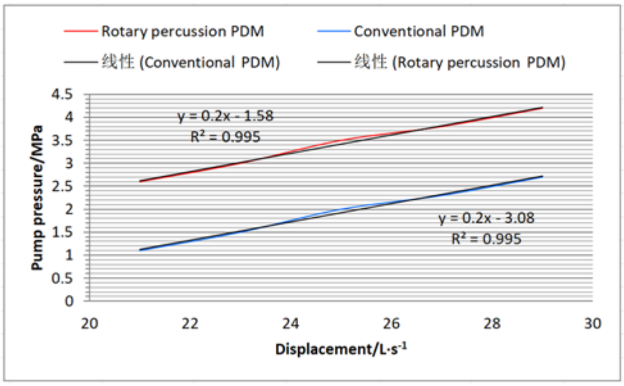

Figure 4. Pump pressure comparison of conventional PDM and RP PDM.

Figure 5 shows the rotating speed and torque contrast of conventional PDM and RP PDM. The two couple of curves have basically overlapped separately, which suggests that the rotating speed and the torque of the conventional PDM and RP PDM is almost the same and that the friction torque consumption is small. Therefore, RP PDM's structure practicability is verified, assembly precision satisfies the requirement of rotating power output, and RP PDM's integral power output characteristic parameters meet the condition requirements of field compound drilling process.

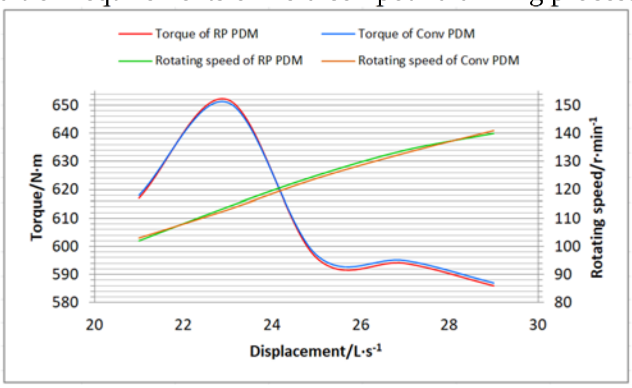

Figure 5. Rotating speed and torque contrast of conventional PDM versus RP PDM.

Test and analysis results show that RP PDM can transform the rotating force of the conventional PDM rotor into the follower's reciprocating impact, which verifies the feasibility of the tool's working principle. Pump pressure for the RP PDM is about 1.5 MPa higher than for conventional PDM. Its toque and rotating speed are almost the same with that of conventional PDM. Friction torque consumption is small and negligible. Except for the lower cam with certain amount of normal wear, the other parts remain in good condition. And the tool's overall power output characteristic parameters meet the condition requirements of field compound drilling process as a result.

5. Field Trials

5.1. Field Trial at Well Xu36A

Well Xu36A is a five-section directional well of "vertical - build up - hold degree - drop degree - hold degree" structure in Jiangsu Oilfield. Its maximum well inclination is 47.5°. There is large frictional resistance in the lower hold degree section of 3112-3985m, with 11° well inclination. This is a well drilled to Paleozoic erathem, which is very rare in oil drilling. The Gaojiabian strata of Silurian in Paleozoic have poor drillability, with drillability grade of about 5-7, which causes great difficulties for the drilling process. RP PDM is taken for trial during the three-open section 3310-3663m of Gaojiabian strata in Xu36A well, tripped out because of the replacement of the straight motor drilling tool.

This well adopts a 1.25 ° RP PDM, whose downhole total working time is 80hs, pure drilling time 54.7hs, total footage 353m, and average ROP 6.45m/h. This well goes into Paleozoic Silurian Gaojiabian strata from 3146m. The stratigraphic lithology of the trial section and the contrastive upper and lower adjacent section are all grey-black mudstone, grey mudstone and light grey shale. Both sections use compound drilling and have strong comparability. ROP comparison between the trial section and the upper and lower adjacent sections is shown in figure 6 and table 1. As can be seen from figure 6 and table 1, ROP of rotary percussion drilling PDM increases by 219% and 132% respectively compared with the upper and lower adjacent sections of the same strata, which reveals good ROP improving effect in hard strata.

Table 1. Comparison of ROP between RP PDM's trial section and adjacent sections of well Xu36A.

Well name	Drilling assembly	Drilling section/m	Stratum	Footage/m	Working hour/h	Average ROP/min·m^{-1}	ROP improvement
Xu36A	T1376BPDC+ bend PDM	3146-3310	Gaojiabian strata	164	81.3	2.02	+219%
	F1653JH PDC+1.25°bend RP PDM	3310-3663		353	54.7	6.45	——
	F1653JH PDC+straight PDM	3663-3843		180	64.8	2.78	+132%

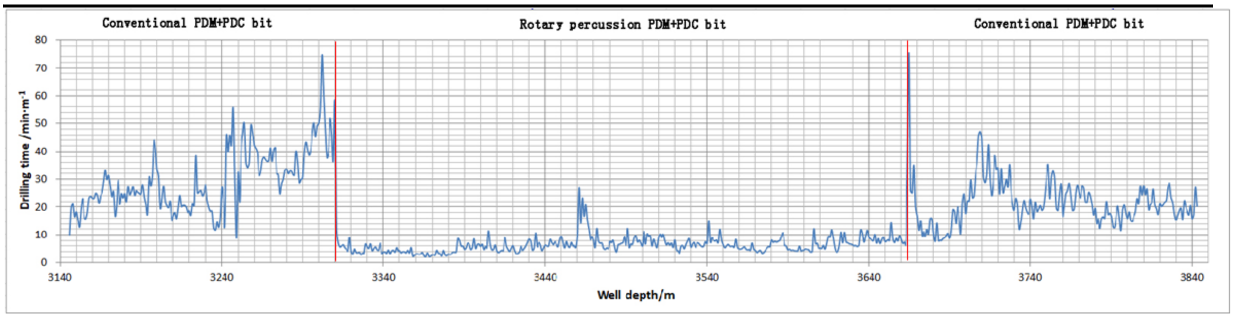

Figure 6. Comparison of drilling hours between RP PDM trial section and adjacent section of well Xu36A.

5.2. Field trial at Well Pan40-Xie511

Pan40-Xie511 is a direction well of second-open structure, shown in figure 7. A 1.5° RP PDM is taken for trial during the second-open section 301-3043m. This section well structure is "vertical - build up - change direction - hold degree", with maximum inclination of 49.2 °, see in figure 6. The tool has been taken trial twice, with a cumulative footage of 2742m and a cumulative working time of 155hs, in which the pure drilling time was 106hs, and the average ROP was 25.87m/ h.

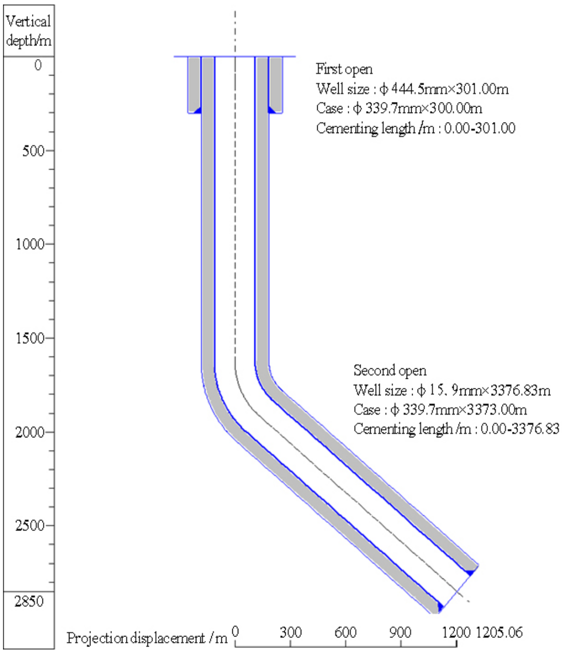

Figure 7. Structure of Well Pan40-Xie511.

In order to evaluate RP PDM's ROP improving effect both in compound drilling and directional drilling more reasonably, ROP of deeper-than-2200m section with the same operating conditions in this well and adjacent well Pan40-Xie412 is compared and analysed. The contrast is shown in table 2 and figure 8. It can be seen from table 2 and figure 8 that the ROP of compound drilling with RP PDM in this well is 41.8% higher and that its sliding drilling ROP is 51.1% higher than that of the adjacent well Pan40-Xie412.

Table 2. Comparison of ROP between well Pan40-Xie511 and well Pan40-Xie412.

Well name	Drilling assembly	Drilling section/m	Drilling mode	Footage/m	Working hour/h	Average ROP/m·h-1	ROP improvement
Pan40-Xie412	PDC+ bend PDM	2200-2819	Compound Sliding	535 65	27.98 25	19.12 2.6	41.80% 51.10%
Pan40-Xie511	PDC+1.5°bend RP PDM	2200-3043	Compound Sliding	806 26	29.72 6.62	27.11 3.9	—— ——

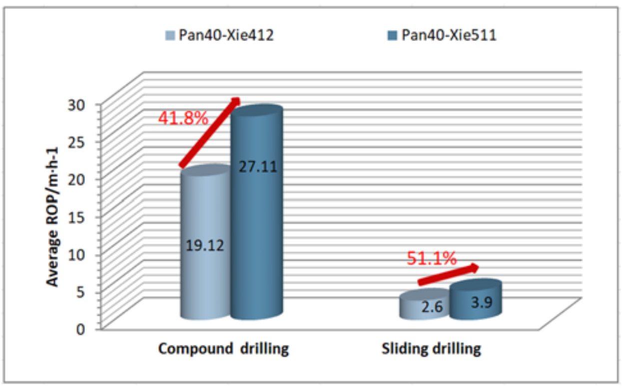

Figure 8. Comparison of ROP between well Pan40-Xie511 and well Pan40-Xie412.

The tool shows good ROP improving and friction-reducing effect in the trials. The directional sliding drilling in the test section is faster than that in the same type directional well of this block, and the tool surface is stable, which effectively eliminates and reduces depressurization phenomenon of the drilling process. The efficiency of orientation is greatly improved as a result.

6. Conclusions

(1)A PDM driven rotary percussion drilling tool is developed. The tool has dual functions such as PDM compound drilling and high frequency impact drilling. It has simple structure and obvious technical advantages.
(2)According to *the Third Strength Theory, the Compressive Stress Condition and the Extrusion Stress Condition*, dangerous sections of the tool are checked and calculated separately and all of them meet the strength requirements.
(3)Engineering prototype of the tool is developed and ground performance test is carried out. The feasibility of its working principle is verified. At the same time, it is shown that the overall dynamic output characteristic parameters of the tool also meet the requirements of the field compound drilling conditions.
(4)Field trials verify that this tool has relatively good ROP improving effect, especially in well Xu36A, ROP is more than doubled in the same strata, which has positive significance for speeding up the exploration and development progress of oil field and reducing drilling cost.
(5)The application of RP PDM in drilling process of directional well can reduce friction of drilling tools, effectively eliminate or alleviate the depressurization phenomenon, and improve the efficiency of directional drilling process. This greatly broadens the tool’s application scope, and lead to very good application prospect consequently.

Acknowledgments

This paper is founded by two projects. The first project is *Development of Mechanical Rotary Percussion drilling tool and Slim Impact Drilling Tool in Complex Drilling Environment* from National Science and Technology Major Project of the Ministry of Science and Technology of China. Its project number is 2016ZX05021-003-002HZ.The second project is *Further Research and Application of Mechanical Rotary Percussion Drilling Tool* from Sinopec Ministry of Science and Technology Management. Its project number is P18001-6.

References

[1] Kexiong Wang. Research and application of percussion rotary drilling technology in petroleum drilling [J]. Oil Drilling & Production Technology,1999,21(5):5-9.
[2] Xiaohua Zhu, Weiji Liu. The rock breaking and ROP rising mechanism for single-tooth high-frequency torsional impact cutting [J]. Acta Petrolei Sinica,2017,38(5):578-586.
[3] Yuanzhou Deng. Feasibility study and exploration on the application of rotary drilling technology in oil drilling [J]. Chemical Enterprise Management,2016,6:171.
[4] Gang Bi, Gensheng Li, Zhan Qu etc. Rock breaking efficiency of the self-propelled swirling jet bit [J]. Acta Petrolei Sinica,2016,37(5):680-687.
[5] Jianming Peng, Kun Yin, Qingyan Wang etc. Mathematical model of liquid pressure in high-pressure chamber of liquid-jet hammer [J]. Journal of the University of Petroleum,China,2005,29(6):50-68.
[6] Kexiong Wang, Yinghu Zhai, Jinglun Cai. Detecting system for hydraulic percusive device [J]. Journal of the University of Petroleum,China,1995,25(2):34-37.
[7] Jinsong Chen, Yinghu Zhai. Mechanical analysis on working process of syzj type of impulsive load generator [J]. Journal of the University of Petroleum,China,2001,25(2):9-14.
[8] Xuecheng Dong, Jiyou Xiong, Guohua Wang etc. Study on running characteristic of oscillation impacter for oil-drilling [J]. Journal of Mechanical Engineering,2014,50(21):197-205.
[9] Xinghua Tao. Present situation and development trend of percussive rotary drilling technology [J]. Drilling & Production Technology,1996,19(1):10-12.
[10] Haiping Zhang, Zhongwei Suo, Hui Zhang etc. The design and experiment of the retaining and sealing mechanism for hydraulic jet hammer [J]. China Petroleum Machinery,2011,39(8):4-6.
[11] Haiping Zhang, Zhongwei Suo, Xinghua Tao. The structural design and experimental study of

the jet-type hydro-hammer [J]. China Petroleum Machinery,2011,39(7):1-3.
[12] Haiping Zhang, Zhongwei Suo, Xinghua Tao. Design of a new type of retaining and sealing mechanism in hydraulic impactor [J]. Oil Field Equipment,2011,40(6):44-47.
[13] Xiaodan Liu, Haiping Zhang, Zhongwei Suo. Failure analysis on rupture cylinder in hydraulic jet hammer [J]. Hot Working Technology,2013,42(3):229-234.
[14] Haiping Zhang, Xiaodan Liu, Zhongwei Suo. Crack analysis on impactor anvil [J]. Hot Working Technology,2013,42(14):201-209.
[15] Haiping Zhang, Zhongwei Suo, Jiachang Wang. Failure analysis on the rupture of a hammer anvil [J]. Journal of Materials Science and Engineering,2013,31(3):468-472.
[16] Haiping Zhang, Jiachang Wang, Deru Qian. Failure analysis and structure improvement of hammer anvil [J]. Journal of Machine Design,2014,31(4):68-71.
[17] Zhongwei Suo, Huibo Yin, Haiping Zhang etc. Application of rotary-percussion drilling technology in yi1 well of inner mongolia [J]. Exploration Engineering (Rock & Soil Drilling and Tunneling),2014,41(3):18-24.
[18] Yunpeng Gen, Dandan Li, Yanfang Fan. Cause analysis and balling prevention of torkbuster drilling tools [J]. Journal of Oil and Gas Technology,2014,36(8):154-158.
[19] Xianglin Zhou, Jincheng Zhang, Dongqing Zhang. Experimental application of torkbuster torsional impactor in yuanba region [J]. Drilling & Production Technology,2011,35(2):15-17.
[20] Guangjun Ma, Jiachang Wang, Haiping Zhang. The design and experimental study of PDM driven rotary percussion drilling tool [J]. Petroleum Drilling Techniques,2016,44(3):50-54.
[21] Guangjun Ma, Haiping Zhang, Jiachang Wang. Designed and testing of the positive displacement motor driven rotary percussion drilling device [J]. China Petroleum Machinery,2016,44(6):24-27.
[22] Haiping Zhang, Xiaodan Liu, Jiachang Wang etc. Structural design and motion simulation research on a new type composite rotary percussion drilling tool [J]. Journal of Mechanical Strength,2017,39(2):392-396.
[23] Gonghui Liu, Yumei Li, Jun Li etc. New technology with composite percussion drilling and rock breaking[J]. Petroleum Drilling Techniques,2016,44(5):10-15.
[24] Cuihong Liu, Tianbing Yuan, Xinyuan Liu. Application of dual drive compound drilling technology in zhongyuan oilfield [J]. Drilling & Production Technology,2004,27(5):98-100.
[25] Peng Lei, Hongjian Ni, Ruihe Wang etc. Field test of self-excited vibration rotary percussion drilling tool in deep and ultra-deep wells [J]. Petroleum Drilling Techniques,2013,41(6):40-43.
[26] Chunyuan Liu, Haichao Jiao, Zhen Chen. Research on the application of rotary drilling technology in oil drilling [J]. Chemical Enterprise Management,2016,11:123.
[27] Hongwen Liu. Material Mechanics [M]. Beijing: Higher Education Press,2004.
[28] Liang Li, Jianzhuang Huang. Test and analysis of hydraulic impactor [J]. Drilling & Production Technology,1996,19(9):51-53.
[29] Zhongwei Suo, Huibo Yin, Haiping Zhang etc. Research on the theory and experiment of cylinder body heating assembly [J]. Mechanical Engineer,2014(4):88-90.